Design of the detection system for the measurement of hyperfine-splitting in μp

L. Sinkunaite[1] on behalf of the CREMA collaboration

[1]Paul Scherrer Institute, PSI Villigen

Proton-radius

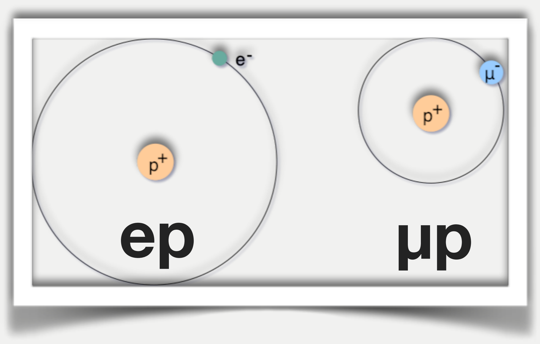

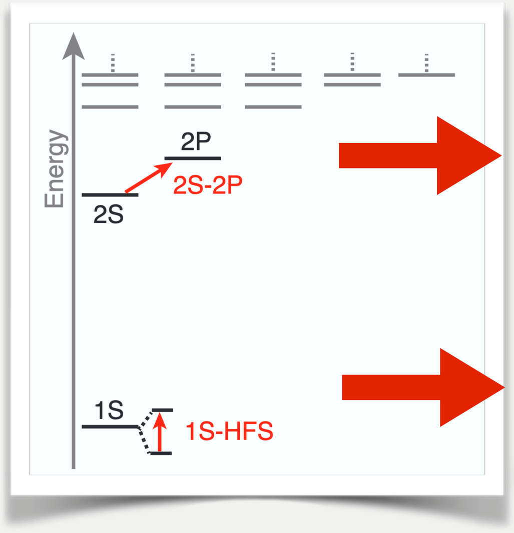

Charge radius

$$< r_p^2 > = -6\hbar^2 \frac{dG_E(Q^2)}{dQ^2}\Big|_{Q^2=0}$$

Zemach radius

$$r_z = -\frac{4}{\pi}\int_0^\infty \frac{dQ}{Q^2}\left[G_E(Q^2)\frac{G_M(Q^2)}{1+\kappa_P} - 1\right]$$

Impact

The experiment is designed to measure the 1S-HFS transition in μp by means of laser spectroscopy with 1 ppm accuracy and to extract the two-photon exchange (TPE) contribution with a relative accuracy of 1 × 10⁻⁴. This would contribute to:

1. *Understanding of the low-energy structure of the proton and providing a benchmark for chiral perturbation theory, for dispersion-based approaches, and for lattice QCD.*
2. *Test of lepton universality: comparison of muonic hydrogen (μp) to electronic hydrogen (ep).*
3. *Development of novel laser technologies.*

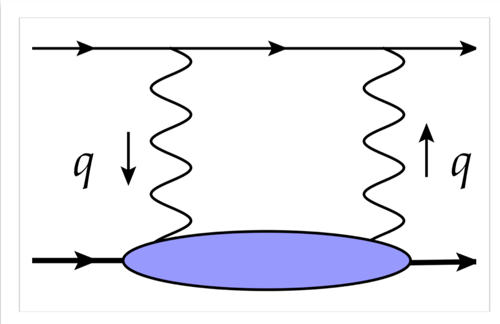

Experimental method

1. **Formation**
   A muon is stopped in hydrogen gas forming a muonic hydrogen (μp) atom in highly excited state.

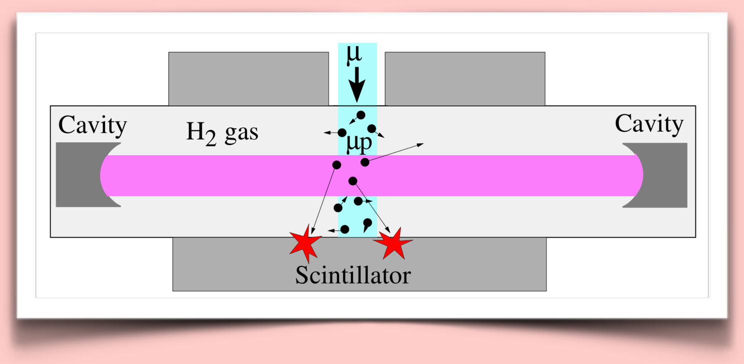

2. **De-excitation**
   The formed μp atom de-excites to the F=0 sub-level of the ground state.
3. **Laser excitation**
   A high-energy laser pulse excited the μp atom from F=0 to F=1,
   $\mu p_{F=0} + \gamma \rightarrow \mu p_{F=1}$.
4. **Collisional de-excitation**
   In a collision with a hydrogen molecule (H_2), the μp atom is de-excited to the F=0 sub-level of the ground state and after ~1 μs is thermalised to the hydrogen gas temperature (50 K),
   $\mu p_{F=1} + H_2 \rightarrow \mu p_{F=0} + H_2 + E_{kin}$.
   The transition energy is converted into the kinetic energy.
5. **Diffusion**
   Having the extra kinetic energy of 0.1 eV, the μp atom efficiently diffuses to the target walls before muon decay occurs.
6. **At the wall**
   At the target wall, which is made of high-Z material, the muon is transferred from the μp to the high-Z material forming (μZ) in an excited state. The highly-excited (μZ)* atoms then de-excite producing MeV X-rays.*

$$\begin{aligned}\mu p + Au \;\rightarrow\; & \mu Au^* + p \\ & \downarrow \\ & \mu Au + \text{X-rays} \\ & \downarrow \\ & \nu + ... + \text{neutrons} + \gamma + p, d, \alpha\end{aligned}$$

7. **Detection**
   The MeV X-rays are detected using scintillators. A resonance is obtained by plotting the number of X-rays versus the laser frequency.

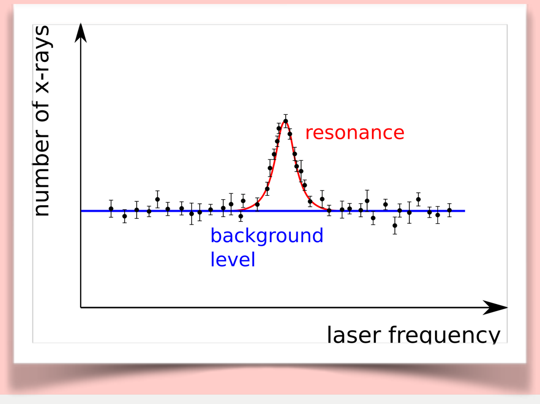

Signal

Signal and background

MeV X-rays detected within a time window Δt.

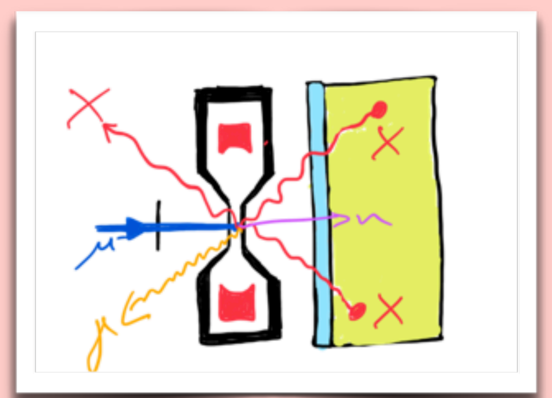

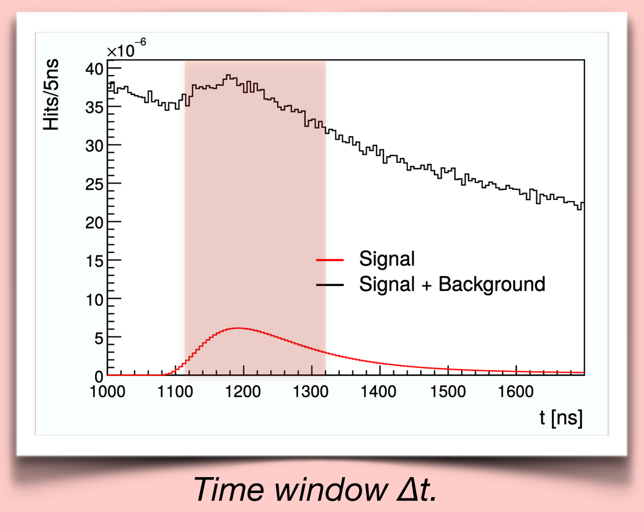

Time window Δt.

Background

Intrinsic:
non-laser excited μp atoms that diffuse to the target walls within Δt.

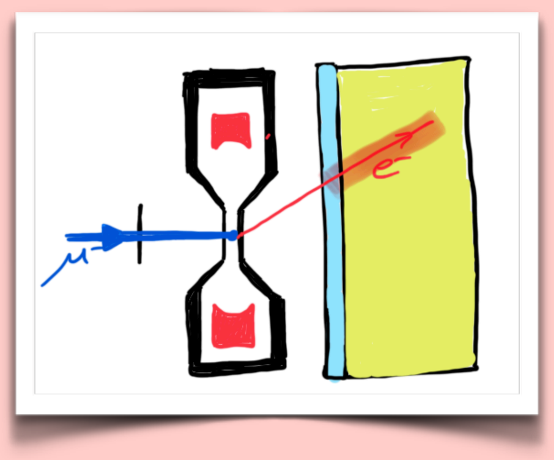

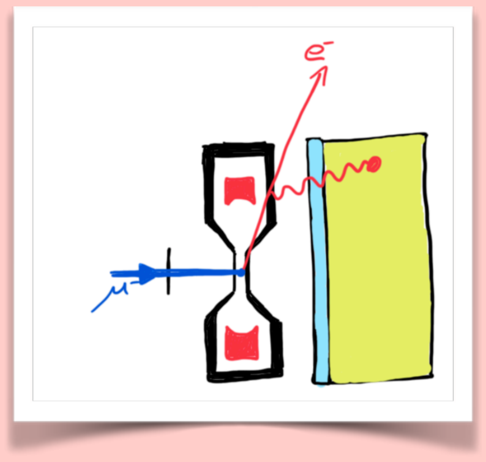

Erroneous:
electrons produced when the muon decays,
$\mu^- \rightarrow e^- \nu_\mu \overline{\nu_e}$,

and erroneously identified as cascade events. This could be caused by bremsstrahlung.

MC simulations

Simulated deposited-energy spectra inside a thin (5-mm) plastic scintillator (above) and inside a thick (250-mm) plastic scintillator (below), for Michel-electrons (red) and X-ray cascade (black).

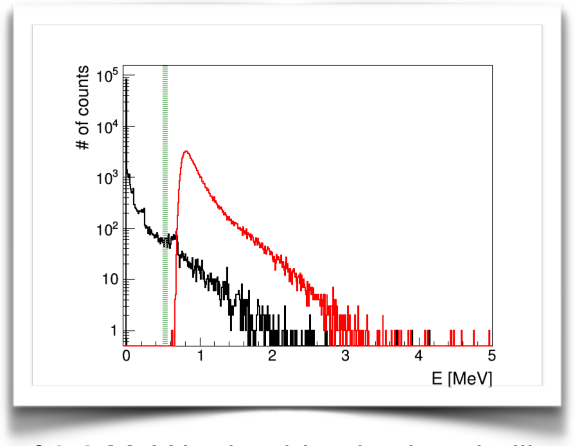

An energy cut of 0.6 MeV in the thin plastic scintillator could be used to distinguish electrons from the X-ray cascades.

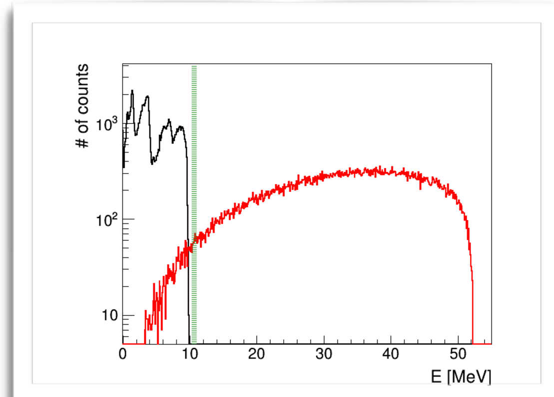

Another energy cut of 10 MeV in the thick scintillator could be used to distinguish high-energy electrons from the X-rays.

- *μAu X-ray cascade*
- *Muon decay ($\mu^- \rightarrow e^- \nu_\mu \overline{\nu_e}$)*
- *Energy threshold*

Detection system

A similar scheme (on the right) to the one that has been studied in the MC simulations. Thin plastic scintillators are shown in yellow, thick plastic scintillators are shown in orange. Blue is showing some shielding material.

Following requirements were taken into account:

1. *High detection efficiency of the (μAu) X-ray cascade events.*
2. *Minimal probability to misidentify the electrons as the cascade events.*
3. *Thin low-Z plastic scintillators and thick high-Z scintillators to minimise the bremsstrahlung effect.*

23 detectors to produce, calibrate, and synchronise!

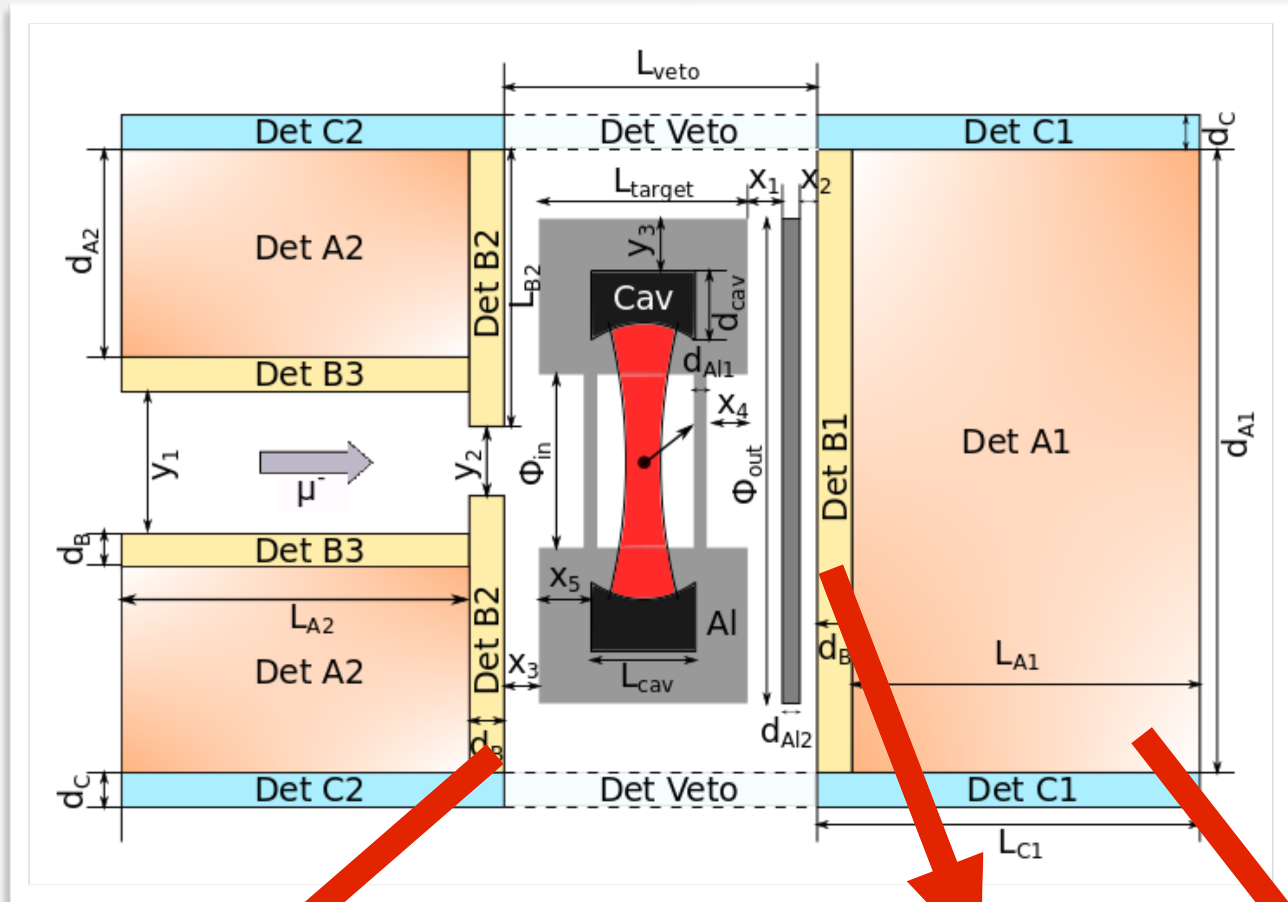

Comparison of target cavity materials

Two target cavities were simulated: one made of copper (high-Z material) and the other made of glass (lower-Z material). The X-ray detection efficiency P_{XX} and the electron misidentification as X-rays P_{eX} were plotted. X-axis depicts the position of the lower threshold on the thick scintillators E_{THR}.

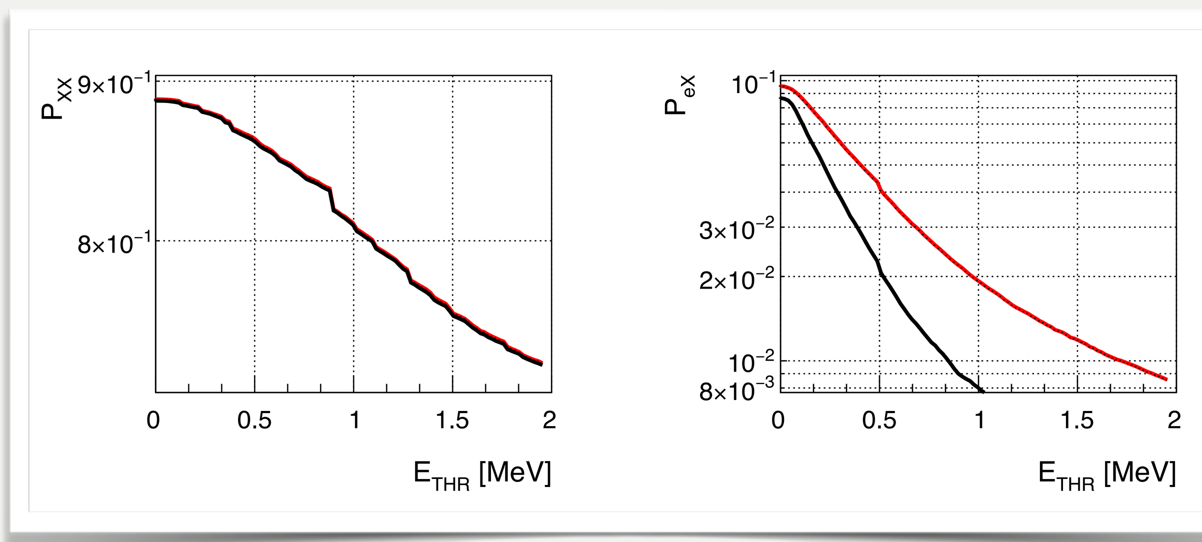

- *Target cavity is made of glass*
- *Target cavity is made of copper*

Wavelength-shifting fibre detectors

Thin (< 10-mm) 250-mm × 250-mm plastic scintillators coupled to the wavelength-shifting fibres and read out with GAPDs are used to distinguish electrons (our background) from μAu X-ray cascades (our signal).

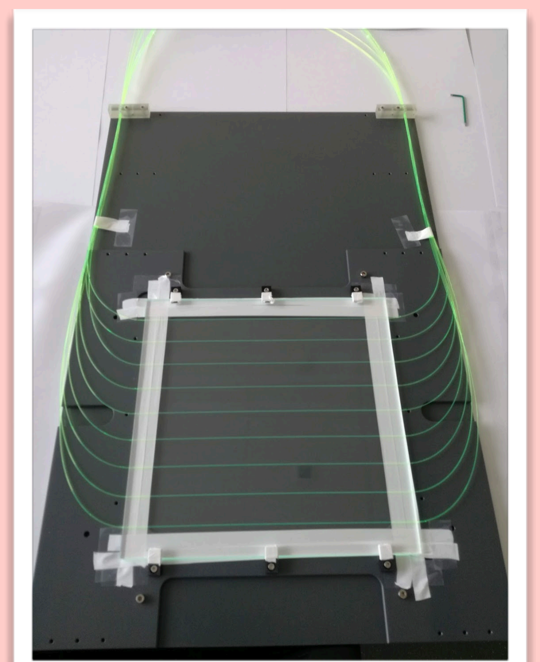

\+

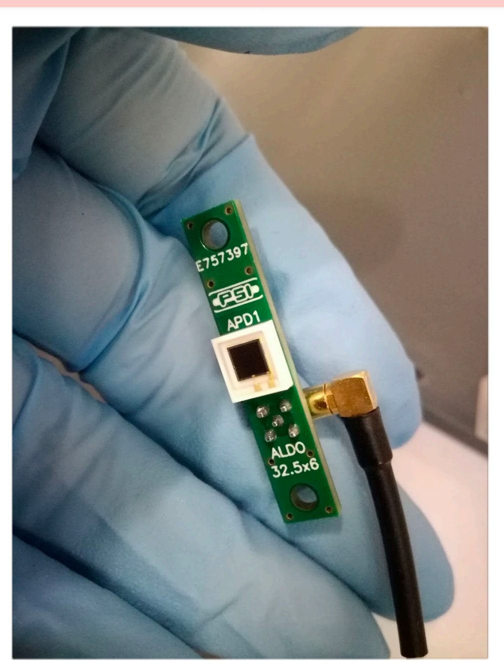

Multi-wire Ar-gas chamber

An alternative detector to the thin-plastic scintillator that can be used to distinguish electron- (our background) from μAu X-ray cascade-event (our signal).

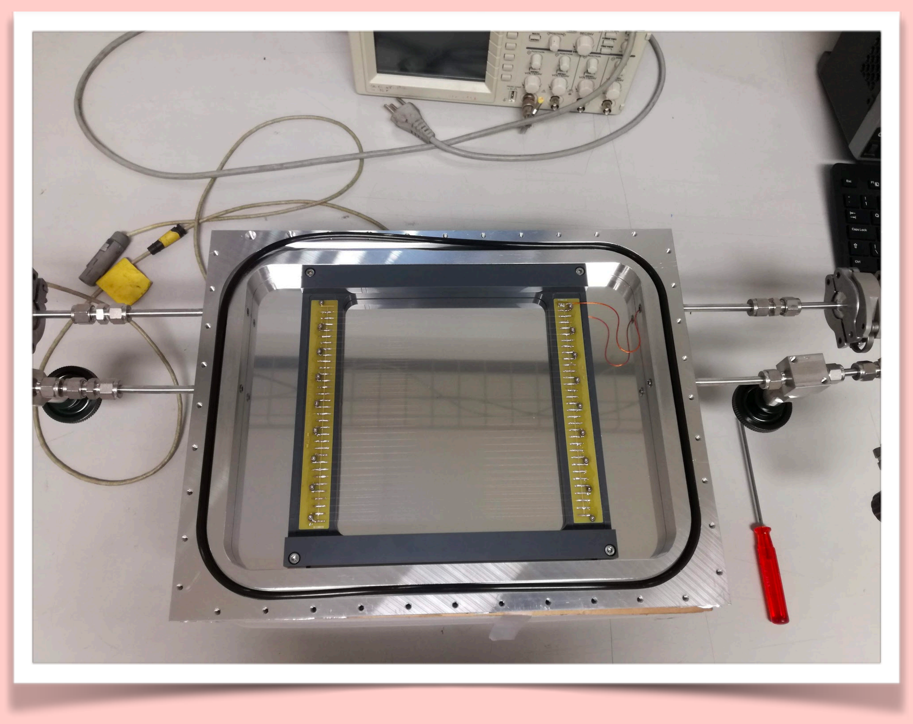

BGO ($Bi_4Ge_3O_{12}$)-crystal detectors

Thick (55-mm) BGO-crystal detectors of 200-mm length read out with PMTs (Photo-multiplier tubes) are used to measure the X-rays (our signal). As an alternative, thick plastic scintillators can be used.